Mechanical feedback enables catch bonds to selectively stabilize scanning microvilli at T-cell surfaces

Robert H. Pullen, III, and Steven M. Abel*
Department of Chemical and Biomolecular Engineering, National Institute for Mathematical and Biological Synthesis, University of Tennessee, Knoxville, TN 37996

ABSTRACT T-cells use microvilli to search the surfaces of antigen-presenting cells for antigenic ligands. The active motion of scanning microvilli provides a force-generating mechanism that is intriguing in light of single-molecule experiments showing that applied forces increase the lifetimes of stimulatory receptor–ligand bonds (catch-bond behavior). In this work, we introduce a theoretical framework to explore the motion of a microvillar tip above an antigen-presenting surface when receptors on the tip stochastically bind to ligands on the surface and dissociate from them in a force-dependent manner. Forces on receptor-ligand bonds impact the motion of the microvillus, leading to feedback between binding and microvillar motion. We use computer simulations to show that the average microvillar velocity varies in a ligand-dependent manner; that catch bonds generate responses in which some microvilli almost completely stop, while others move with a broad distribution of velocities; and that the frequency of stopping depends on the concentration of stimulatory ligands. Typically, a small number of catch bonds initially immobilize the microvillus, after which additional bonds accumulate and increase the cumulative receptor-engagement time. Our results demonstrate that catch bonds can selectively slow and stabilize scanning microvilli, suggesting a physical mechanism that may contribute to antigen discrimination by T-cells.

INTRODUCTION

T-cells directly engage antigen-presenting cells (APCs) to search for surface-displayed antigens. They use the T-cell receptor (TCR) complex to discriminate between self and foreign ligands in the form of peptides presented by major histocompatibility complex (pMHC) molecules on the APCs. T-cells are able to recognize small numbers of antigens among a vast number of self-pMHCs (Sykulev *et al.*, 1996; Huang *et al.*, 2013; Pageon *et al.*, 2016) while being sensitive enough to distinguish between peptides with a single amino acid

difference (Hogquist *et al.*, 1994; Robbins *et al.*, 2008). However, a comprehensive understanding of the mechanisms governing antigen recognition remains elusive, and growing evidence points to the importance of mechanical forces at the T-cell–APC interface (Depoil and Dustin, 2014; Hivroz and Saitakis, 2016; Upadhyaya, 2017).

Recent experiments have revealed two intriguing physical mechanisms related to antigen recognition: 1) T-cells use microvillar protrusions to actively search APCs, suggesting a mechanism to scan large portions of the APC surface (Cai *et al.*, 2017). 2) The average lifetime of a bond between a TCR and an antigenic pMHC is maximized when there is an applied force on the TCR-pMHC complex (Liu *et al.*, 2014; Das *et al.*, 2015). Taken together, these results suggest feedback between microvillar motion and TCR-pMHC binding: Forces imparted by microvillar motion influence TCR-pMHC lifetimes, while tensions on individual TCR-pMHC complexes impact microvillar motion. To our knowledge, this feedback and its consequences have not been explored before.

Microvilli are fingerlike membrane protrusions that have been observed on T-cells in a variety of studies (Sage *et al.*, 2012; Hivroz and Saitakis, 2016; Jung *et al.*, 2016; Cai *et al.*, 2017; Kim *et al.*, 2018;
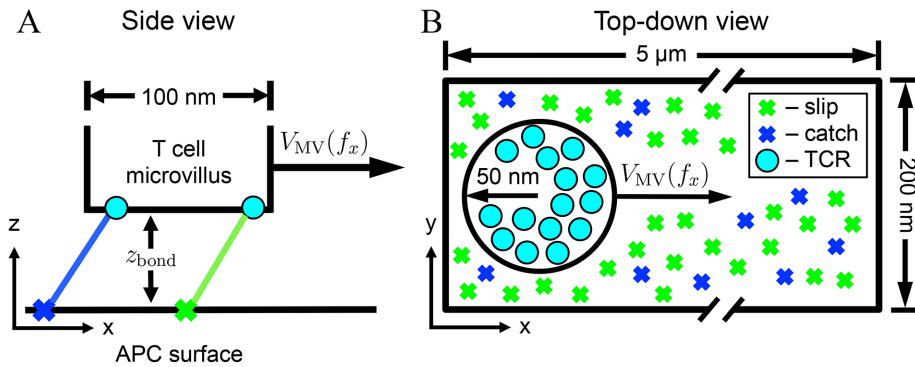
FIGURE 1: Schematic of a T-cell microvillus scanning across the surface of an APC. TCR-pMHC bonds stochastically form and dissociate as the microvillus moves across the APC surface. The velocity, V_{MV}, depends on the force exerted on the microvillar tip by TCR-pMHC complexes. (A) Side view of the system with the T-cell microvillar tip residing above the APC surface. (B) Top-down view. The microvillus moves in the x direction. A mixed population of pMHCs is shown; some form catch bonds upon binding TCRs, while others form slip bonds.

Razvag *et al.*, 2018). They also contain large numbers of highly localized TCRs (Jung *et al.*, 2016; Kim *et al.*, 2018), and a recent study using lattice light-sheet microscopy revealed that T-cells use microvilli to actively scan the surfaces of APCs (Cai *et al.*, 2017). Interestingly, this study showed that cognate pMHC on the APC resulted in some microvilli becoming "stabilized," with long-lived contact at localized regions on the APC surface. This stabilization occurred even when early intracellular signaling through the TCR was disrupted, suggesting that a physical mechanism might be responsible. Taken together, these studies suggest that microvilli play a role in antigen discrimination during early stages of T-cell activation.

Physical contact between the T-cell and APC leads to mechanical forces at the cell–cell interface. TCR-pMHC complexes experience forces that arise from a variety of sources, including cell motion, membrane undulations, active cytoskeletal processes, and the microvillar motion described earlier (Hivroz and Saitakis, 2016; Pullen and Abel, 2017). A number of recent experimental studies have characterized the force dependence of TCR-pMHC dissociation kinetics (Huang *et al.*, 2010; Depoil and Dustin, 2014; Liu *et al.*, 2014; Das *et al.*, 2015; Hong *et al.*, 2015, 2018; Feng *et al.*, 2017; Sibener *et al.*, 2018). When bound to stimulatory pMHC, the TCR exhibits catch-bond behavior, in which the average lifetime is maximized when a force ~10–20 pN is applied to the protein complex. In contrast, a TCR bound to a nonstimulatory pMHC exhibits slip-bond behavior, in which the lifetime strictly decreases with increasing force. The ligand and force dependence of the dissociation kinetics has been proposed as a potential mechanism to enhance discrimination between self- and foreign pMHC (Liu *et al.*, 2014; Feng *et al.*, 2018).

In this paper, we investigate the mechanical coupling between microvillar motion and TCR-pMHC binding. We are interested in whether the interplay between the two provides a physical mechanism that could impact antigen recognition. To this end, we introduce a physically motivated theoretical framework describing the motion of a microvillus near an antigen-presenting surface. The framework captures key biophysical features while being simple enough to analyze in detail. When possible, we use experimentally derived parameters, including those for force-dependent TCR-pMHC dissociation kinetics. In the *Results*, we first characterize the motion of scanning microvilli in the presence of surfaces containing

nonstimulatory (slip) pMHC, stimulatory (catch) pMHC, and mixtures of the two. We characterize the distribution of microvillar velocities for different cases and assess when an individual microvillus has stopped. We then characterize the total time of receptor engagement as a proxy for the degree of stimulation of TCRs at the microvillar tip. We conclude by discussing some assumptions of the model, the physical picture that emerges from our simulations, and potential implications for antigen recognition by T-cells.

METHODS

We consider a theoretical framework in which an isolated microvillus scans across an antigen-presenting surface. The velocity of the microvillus depends on the forces exerted on the microvillus by TCR-pMHC complexes ("bonds"). The number of bonds, bond lifetimes, and microvillar velocity are dependent on the interplay between stochastic binding and dissociation events, diffusive processes, and forces that result from the stretching and compression of bonds by the moving microvillus. We use a stochastic reaction–diffusion framework that accounts for the microvillar motion and the forces on TCR-pMHC bonds.

Computational framework

Figure 1 provides a schematic depiction of the model. We represent a patch of the antigen-presenting surface as a rectangular domain in which pMHC molecules diffuse (Capps *et al.*, 2004). The tip of the T-cell microvillus is represented by a circular surface with a diameter of 100 nm (Majstoravich *et al.*, 2004; Fisher *et al.*, 2008; Jung *et al.*, 2016; Razvag *et al.*, 2018). We assume that it resides at a fixed distance above the antigen-presenting surface, which we take to be the length of a TCR-pMHC complex (z_{bond}). TCRs diffuse about the microvillar tip and bind to pMHC molecules on the antigen-presenting surface. TCRs and pMHCs are represented by particles with a 5-nm radius (Birnbaum *et al.*, 2014), and particles on the same surface cannot overlap due to excluded volume. Although adhesion molecules such as LFA-1 play a role in T-cell activation (Springer, 1990), it has been shown that LFA-1 and its binding partner ICAM-1 are excluded from the region between the tip of a microvillus and the antigen-presenting surface (Cai *et al.*, 2017). Therefore, we do not include these molecules in our model, which focuses just on the tip of the microvillus and not on other parts of the T-cell surface.

When TCR-pMHC bonds are stretched relative to their natural length, they impose a force on the microvillus. We describe the force with a linear spring model, $f = k_{bond} (L - z_{bond})$, where k_{bond} is the spring constant, L is the distance between the two bound particles, and the force is directed along the bond. Experiments have shown that the intracellular domain of an MHC molecule impacts its motion, likely by interactions with the cortical actin cytoskeleton, and that shortening the intracellular domain leads to faster diffusion (Edidin *et al.*, 1991; Kwik *et al.*, 2003; Capps *et al.*, 2004). After a pMHC binds to a TCR, we assume that interactions with the cytoskeleton interfere with its motion. In our model, this interference completely arrests the motion of the MHC molecule, and as a consequence, the TCR-pMHC complex can sustain dynamically changing forces.

The microvillar tip moves across the antigen-presenting surface in the x direction. In the absence of an external force, the microvillus moves at velocity V_0. However, forces arising from TCR-pMHC bonds impact the microvillar velocity, which we assume depends linearly on the component of the net force in the x direction, $f_x(t)$:

$$V_{MV}(t) = V_0 \left(\frac{f_{MV} + f_x(t)}{f_{MV}} \right) \tag{1}$$

Here, f_{MV} is a characteristic force, and the time dependence of f_x is a consequence of the formation, stretching, and breaking of bonds. We assume that active processes driving the microvillus keep it in close apposition to the APC surface, and thus we neglect motion in the z direction. Additionally, we ignore velocity fluctuations in the y direction, as these would average to zero and can be thought of as changing the frame of motion of the microvillus. Physically, for an individual TCR-pMHC bond, when the pMHC is "in front of" the TCR ($x_{pMHC} > x_{TCR}$), it effectively pulls the microvillus forward and increases the velocity. When the pMHC is "behind" the TCR, it decreases the velocity. The linear dependence of the velocity on force is consistent with the terminal velocity of an object experiencing a viscous drag. We discuss this choice and the results of a different functional form for V_{MV} later in the paper.

We use a discrete-time, continuous-space stochastic algorithm to describe the dynamics of the system. During each time step, the algorithm accounts for diffusive hops of particles, binding events, and dissociation of bonds. At the end of each time step, the position of the microvillus is updated in accordance with its velocity, which impacts the state of the system by changing the lengths of TCR-pMHC bonds and the positions of TCRs relative to the antigen-presenting surface. Details of the algorithm are presented in the Supplemental Material.

Parameters used in the model are summarized in Table 1. The system size is 200 nm × 5 µm, which is sufficiently long for the microvillar tip to remain within the domain. The total pMHC concentration is fixed at 100 pMHC/µm² (Grakoui et al., 1999; Casal et al., 2005; O'Donoghue et al., 2013), and the microvillar tip contains 23 TCRs (Jung et al., 2016). Results presented in this paper use the diffusion coefficients in Table 1. Additional results with varied diffusion coefficients are shown in the Supplemental Material. The state of the system is recorded every 2.5×10^{-4} s. The computer simulation code is available in the Open Science Framework repository at osf.io/bgqfj.

TCR-pMHC binding kinetics

In the model, TCR-pMHC dissociation kinetics are described by the Bell model for slip bonds (nonstimulatory pMHCs) and by the two-pathway model for catch bonds (stimulatory pMHCs). The off-rate in the Bell model is characterized by (Bell, 1978)

$$k_{off}^{slip}(f) = k_0 \, e^{f/f_0} \tag{2}$$

where k_0 is the off-rate at zero applied force, f is the force on the receptor-ligand complex, and f_0 is the reference force. The off-rate in the two-pathway model is characterized by (Pereverzev et al., 2005)

$$k_{off}^{catch}(f) = k_c e^{-f/f_c} + k_s e^{f/f_s} \tag{3}$$

where c and s denote catch- and slip-phase parameters, respectively.

We parameterized experimental bond-lifetime data from two previous studies. Liu and colleagues used a biomembrane force probe to characterize the interactions of the OT1 TCR with a panel of pMHCs that ranged from a nonstimulatory peptide (E1) to a strongly stimulatory peptide (OVA) (Liu et al., 2014). Feng and coworkers used optical tweezers to investigate interactions of the N15 TCR with the stimulatory vesicular stomatitis virus octapeptide (VSV8) presented by the MHC class I molecule H-2Kᵇ (Feng et al., 2017). Figure 2 shows the average bond lifetime as a function of tensile force for the cases we consider in this paper. We also consider a hypothetical slip bond ("strong slip") with the same maximum lifetime as a VSV8 catch bond and the same reference force as the E1 slip bond. The strong slip bond is used as a control to determine whether a slip bond with a large zero-force lifetime behaves similarly to the catch-bond cases. For convenience, we refer to the two catch bonds and the strong-slip bond as "stimulatory." Parameters for the different cases are tabulated in Supplemental Table S1.

To characterize binding rates, we use data from Huang et al. (2010), who reported effective two-dimensional on-rates for the OT1 TCR binding to OVA and to E1 pMHC (Table 1). We use the on-rate reported for OVA to describe the binding of all stimulatory pMHC in this study (OVA, VSV8, and "strong slip").

RESULTS

In this section, we characterize the collective effects of catch and slip bonds on the motion of microvilli. The total pMHC concentration is fixed at 100 µm⁻² throughout. For reference, we consider an

Variable	Definition	Value	Units	Source
D_{pMHC}	Diffusion coefficient, pMHC	3×10^{-3} (varied)	[µm²/s]	Wofsy et al., 2001; Capps et al., 2004
D_{TCR}	Diffusion coefficient, TCR	0.01 (varied)	[µm²/s]	Favier et al., 2001; Brameshuber et al., 2018
Δr	Diffusive step length	10	[nm]	—
V_0	Microvillar velocity, no force	5.2	[µm/min]	Cai et al., 2017
f_{MV}	Threshold force, microvillar velocity	50	[pN]	—
k_{bond}	Compressional stiffness of bonds	1	[pN/nm]	Pullen and Abel, 2017
$k_{nonstim}^{on}$	2D on-rate, nonstimulatory pMHC	2.6×10^2	[nm²/s]	Huang et al., 2010
k_{stim}^{on}	2D on-rate, stimulatory pMHC	2.4×10^5	[nm²/s]	Huang et al., 2010
z_{bond}	TCR-pMHC complex length	13	[nm]	Springer, 1990
Δt	Time step	2.5×10^{-5}	[s]	—

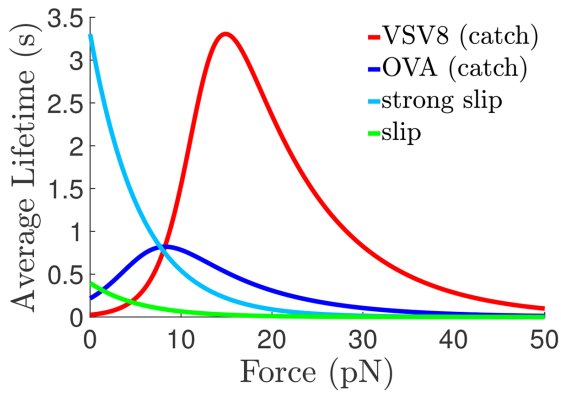**TABLE 1:** Parameters used in the model.

FIGURE 2: Average TCR-pMHC lifetimes as a function of tensile force. Curves for VSV8, OVA, and slip were fitted using nonlinear least-square fits of experimental data from Liu *et al.* (2014) and Feng *et al.* (2017). The "strong slip" bond is a hypothetical control with the same maximum average lifetime as VSV8 and the same reference force as the slip bond.

antigen-presenting surface containing only nonstimulatory ligands with slip-bond kinetics. We then mimic varying degrees of stimulation by replacing 10, 20, 30, and 100% of the nonstimulatory pM-HCs with stimulatory pMHCs (either VSV8, OVA, or strong slip). Cai and coworkers showed that multiple scanning microvilli were able to cover 98% of an APC surface within 1 min (Cai *et al.*, 2017), so we simulate each microvillar trajectory for 60 s. For each condition, we generate 25 independent trajectories to assess stochastic effects.

Scanning microvilli are slowed in a ligand-dependent manner
Figure 3 shows the average microvillar displacement over time for the three different stimulatory pMHCs at various fractions of the total concentration. The green line (0% stimulatory pMHC) represents the average microvillar position when only nonstimulatory slip bonds are present. For this case, the average displacement grows linearly in time with a velocity of 3.5 µm/min, which is less than the zero-force velocity of the microvillus ($V_0 = 5.2$ µm/min). From Eq. 1, the average velocity is consistent with the nonstimulatory TCR-pMHC bonds exerting an average net force of ~16 pN in the direction opposed to the microvillar motion.

The average displacement of the microvillus decreases as the fraction of stimulatory pMHCs increases. VSV8 leads to the most pronounced decrease in microvillar displacement, with increasing

fractions of VSV8 leading to slower average microvillar movement. For 100% VSV8, the average displacement is nearly completely arrested after a short time. OVA generates similar behavior with smaller relative changes as the fraction of OVA is changed. The strong-slip case shows the weakest change in the average displacement as its fraction increases.

Supplemental Figure S1 shows results for varied diffusion coefficients and various fractions of VSV8. For faster diffusion, when only slip bonds are present (0% VSV8), the average microvillar displacement is similar to the result for 0% VSV8 in Figure 3. However, when VSV8 is present, the average microvillar displacement is slower than the corresponding case in Figure 3. For completely immobilized pMHC ($D_{pMHC} = 0$ µm²/s), the average microvillar motion is faster. For all diffusion coefficients, the trend is the same, with the average displacement decreasing as the fraction of VSV8 pMHC increases.

T-cells can identify antigenic pMHCs at concentrations as low as 1 agonist/µm² (Sykulev *et al.*, 1996; Huang *et al.*, 2013; Pageon *et al.*, 2016). In our simulations, this corresponds to a single stimulatory pMHC (1%). At this concentration, encounters between a TCR and stimulatory pMHC are relatively rare. With slow pMHC diffusion, the average microvillar displacement is almost indistinguishable from the case with 0% stimulatory pMHC (Supplemental Figure S1). However, faster pMHC diffusion increases the likelihood of encountering the stimulatory pMHC, leading to slower average microvillar motion.

Heterogeneity of microvillar trajectories
Stochastic binding and dissociation events lead to differences in the motion of microvilli even at identical conditions. Figure 4 shows the time-dependent positions of microvilli from multiple independent simulations. When only nonstimulatory pMHCs are present (Figure 4A), there is relatively small variation between individual displacements. However, when the fraction of VSV8 pMHC is 10%, there is markedly more variation between individual microvillar trajectories. One particularly striking feature is that some trajectories plateau for sustained periods of time. During these periods, the microvillus is approximately stationary due to forces exerted by TCR-pMHC bonds. When the fraction of VSV8 pMHC is 30%, a greater fraction of microvilli become effectively immobile within the 1-min period, which further decreases the average microvillar displacement. Analogous figures with OVA and strong-slip pMHC are shown in Supplemental Figure S2.

Supplemental Movies S1 and S2 show sample trajectories at 10 and 30% VSV8 pMHC, respectively. In each, the microvillus experiences a period during which it is nearly stationary. For these cases, it can be seen that binding a small number of catch bonds
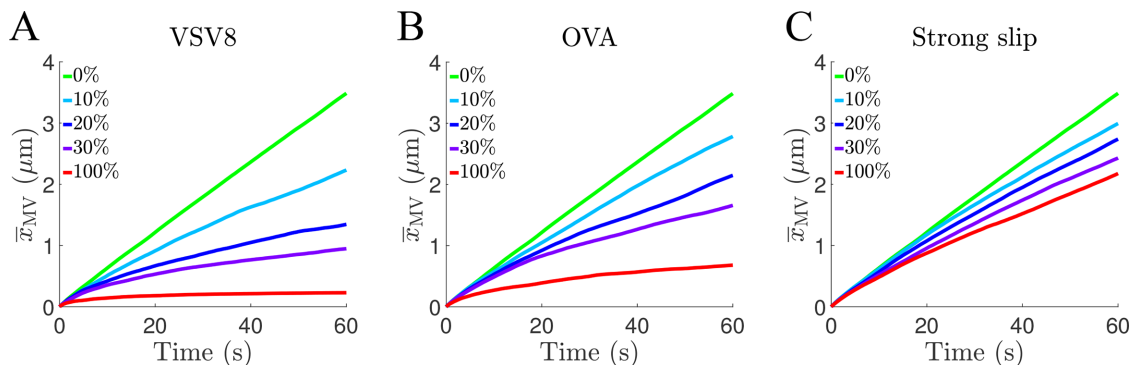

FIGURE 3: Average microvillar displacement for different fractions of stimulatory pMHC: (A) VSV8, (B) OVA, and (C) strong slip. Each line shows the average displacement from 25 independent trajectories.
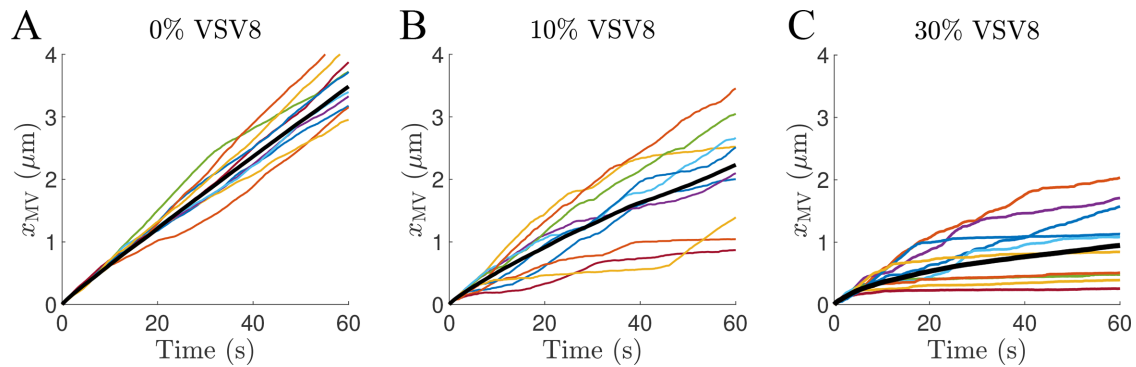
FIGURE 4: Displacements of microvilli for (A) nonstimulatory pMHC, (B) 10% VSV8 pMHC, and (C) 30% VSV8 pMHC. Black lines show the average microvillar displacement calculated from 25 independent trajectories. Colored lines show the displacements of individual microvilli (10 shown).

significantly impacts the velocity of the microvillus. Once the catch bonds significantly slow the microvillus, additional slip bonds accumulate over time.

Catch bonds stabilize microvilli

Figure 5 characterizes distributions of the microvillar velocity for different types and fractions of stimulatory pMHC. When only nonstimulatory pMHCs are present (green line), the velocity distribution is approximately normal with a velocity of 3.48 ± 1.08 μm/min (mean ± SD). Figure 5A shows how the presence of VSV8 pMHC changes the velocity distributions. At 10% VSV8, a small peak in the probability density emerges near 0 μm/min, which is associated with stationary ("stabilized") microvilli. As the fraction of VSV8 increases, both the number and duration of immobile microvilli increase, leading to more prominent and narrower peaks. Results for OVA (Supplemental Figure S3) are similar but less pronounced. Figure 5B compares distributions of the velocity for systems containing varied fractions of strong-slip pMHC. Although larger fractions of strong-slip pMHC decrease the average velocity, in contrast with Figure 5A, the velocities extend across a broad range with no peak near 0 μm/min. Thus, even large fractions of strong-slip pMHC do not result in the effective immobilization of microvilli.

To further characterize the stabilization of microvilli by stimulatory pMHC, we examine the probability that a microvillus effectively stops during the course of a simulation (Figure 6). We define a

"stopping event" to be when a microvillus has an average velocity ≤0.25 μm/min for a continuous period of at least 10 s. Varying the thresholds for the average velocity and the time interval did not affect our conclusions. Figure 6 shows that the microvillus did not stop for any fraction of strong-slip pMHC. However, stopping does occur when stimulatory pMHC with catch-bond characteristics (OVA and VSV8) are present. For OVA, stopped microvilli are observed at 20% OVA, and there is a significant increase in the number of stopped microvilli at larger fractions of OVA. For VSV8, stopped microvilli are observed at all fractions of VSV8, with larger fractions increasing the likelihood of stopping.

Catch bonds impact cumulative TCR-pMHC binding times

In Figure 7, we examine the time-dependent displacement of a microvillus in conjunction with the number of slip and catch bonds. Figure 7A shows a case with only nonstimulatory pMHC present. Although the number of slip bonds varies during the simulation, the slope of the microvillar displacement remains relatively constant. This is consistent with a rapid turnover of bonds, in which they frequently form and break (see Supplemental Table S2). Figure 7, B and C, shows cases with 10 and 30% VSV8 pMHC, respectively. These two figures correspond to Supplemental Movies S1 and S2. In both cases, when two or more catch bonds form, the microvillus slows dramatically. After the microvillus is initially stabilized, there is a gradual ac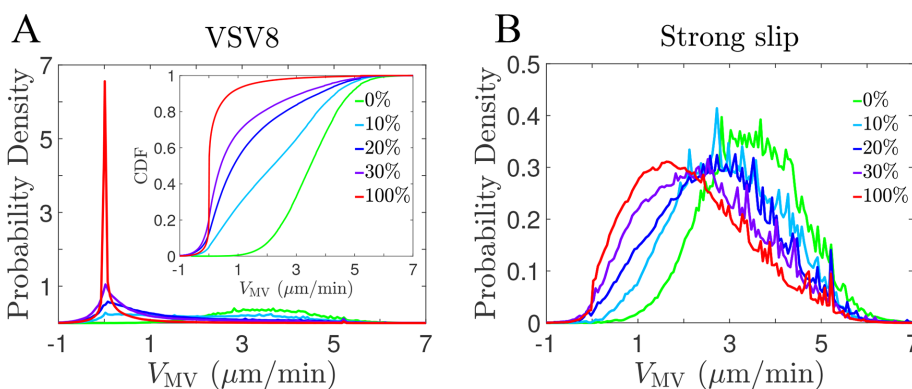cumulation of additional slip bonds. In Figure 7B, the sudden increase in velocity at later time points is coincident with the breaking of catch bonds and a rapid decrease in the number of slip bonds. Supplemental Figure S4 shows the average number of catch and slip bonds as a function of microvillar velocity. These results are consistent with TCR-pMHC bonds accumulating at stabilized microvilli: In systems with catch bonds, slower velocities have more TCR-pMHC bonds on average.

Our results indicate that catch bonds selectively stabilize scanning microvilli in a stochastic manner and that TCR-pMHC bonds accumulate when the microvillus is stopped. This suggests a physical mechanism that could link the motion of the microvillus to intracellular processes through receptor engagement. As a proxy for the degree of stimulation through the TCR, we calculate

FIGURE 5: (A) Probability density and cumulative distribution function (inset) of the microvillar velocity for various fractions of VSV8 pMHC. (B) Probability density of the microvillar velocity for various fractions of strong-slip pMHC. Each distribution is constructed from the velocities obtained over the course of 25 independent trajectories. The green curve (0%) is the same on both figures.
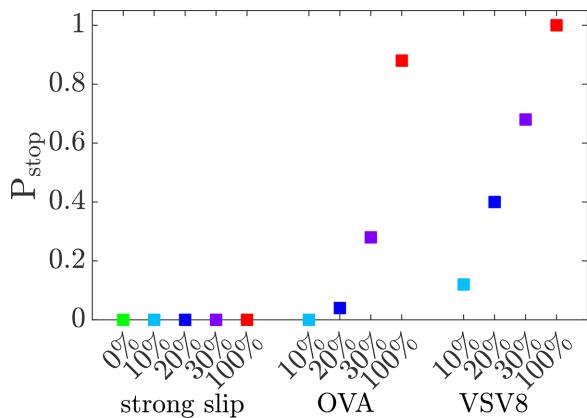
FIGURE 6: Probability that a microvillus is immobilized ("stops") within 1 min of scanning. A "stopping event" occurs when the average velocity is ≤0.25 μm/min for a continuous period of at least 10 s. Each point is obtained from 25 independent trajectories.

the cumulative time of receptor engagement as a function of time for each trajectory:

$$\text{Time engaged}(t) = \sum_{i=1}^{n_{\text{bonds}}} (t - t_{i,0}) \qquad (4)$$

Here, n_{bonds} is the number of bound TCRs at time t and $t_{i,0}$ is the time of bond formation for a given TCR-pMHC complex. Thus, at time t, this function gives the total time that all current TCR-pMHC complexes have been present. Given the results on microvillar stopping in Figure 6, we analyze trajectories with and without stopping

events separately to provide insight into the effects of microvillar stabilization by catch bonds.

When only nonstimulatory slip bonds are present, the average cumulative time of engagement is 0.26 s. Figure 8A shows the average time of engagement for trajectories with a microvillus-stopping event for various fractions of VSV8 pMHC. The average time engaged increases with increasing fraction of stimulatory pMHC, exceeding 10 s for 30% VSV8. Note that these curves underestimate the typical time engaged for a specific stabilized microvillus, because the average occurs over periods in which some microvilli are stopped and others are not. In comparison, Figure 8B shows a substantially smaller average time engaged for trajectories in which the microvillus does not stop. Figure 8C shows the average time engaged for systems with various levels of strong-slip pMHC, which did not induce any stopping events. The time engaged increases with an increasing fraction of strong-slip pMHC, but in all cases, the time engaged is substantially lower than corresponding cases in which catch bonds resulted in a stopping event (Figure 8A). Thus, systems with catch bonds are able to generate much longer sustained receptor engagement in comparison with even the strong-slip system.

DISCUSSION
In this paper, we introduced a theoretical framework to explore the motion of a T-cell microvillus scanning across the surface of an antigen-presenting cell. TCRs at the tip of the microvillus interact with pMHCs on the antigen-presenting surface, and mechanical forces on the TCR-pMHC complexes resulting from motion of the microvillus impact both TCR-pMHC lifetimes and the microvillar velocity. Using parameters obtained from experimental studies of T-cells, we
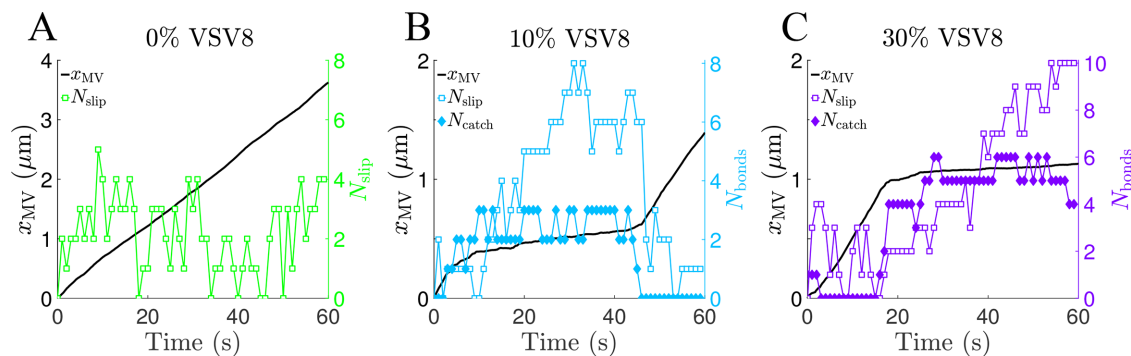

FIGURE 7: Number of catch and slip bonds (colored lines, right axes) and the microvillar displacement (black lines, left axes) for sample trajectories at three fractions of VSV8 pMHC (A–C).
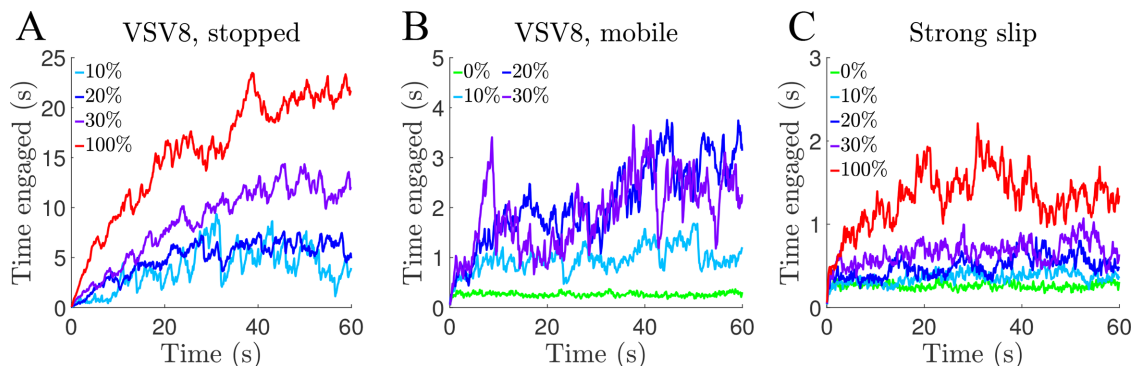

FIGURE 8: Average cumulative time of receptor engagement for various systems: (A) VSV8 on microvilli with stopping events, (B) VSV8 on microvilli without stopping events, and (C) strong-slip pMHC. No stopping events were observed for the strong-slip case.

showed that relatively small numbers of stimulatory pMHCs with catch-bond characteristics immobilized microvilli in the model through the mechanical coupling of microvillar motion and TCR-pMHC binding. In contrast, slip bonds alone did not immobilize microvilli. These results are demonstrated by Figures 5 and 6, which show the distribution of velocities for scanning microvilli and the likelihood that a microvillus becomes immobilized. Microvillar immobilization becomes more prevalent as the concentration of antigenic pMHC increases.

Choice of the velocity profile, V_{MV}

The mechanisms underlying microvillar motion on T-cells have not been fully elucidated experimentally (Majstoravich *et al.*, 2004; Burkhardt *et al.*, 2008; Cai *et al.*, 2017). As such, we chose to use a simple, physically motivated model relating microvillar velocity to the force on the microvillus. Our model uses a linear relationship between the velocity, V_{MV}, and the applied force in the direction of motion. This relationship is consistent with the terminal velocity (zero acceleration) of an object experiencing a viscous drag: $F_A + f_x - \mu V_{MV} = 0$. Here, F_A is a constant applied force driving the motion of the object (provided, for example, by cytoskeletal processes within the cell), f_x is the applied force due to bonds, and μ is the drag coefficient relating the velocity to the drag force μV_{MV}. Thus, $V_{MV} = (F_A + f_x)/\mu$, which is consistent with Eq. 1.

The characteristic force in Eq. 1, f_{MV}, is unknown. If f_{MV} is too small, then even single slip bonds would significantly slow the microvillus. If f_{MV} is too large, then even a large number of bonds would not be able to significantly slow the microvillus. Both of these limits are inconsistent with the results from Cai *et al.* (2017). With these limits in mind, we chose the value to be a few times larger than both typical forces experienced by individual TCR-pMHC bonds (Liu *et al.*, 2016) and the force associated with the peak lifetime for catch bonds (Liu *et al.*, 2014; Das *et al.*, 2015). Moderately changing the value of f_{MV} impacts quantitative aspects of our results, although it does not impact the observation that catch bonds selectively stabilize microvilli. Supplemental Figure S5 shows this for twofold changes in the force threshold for purely stimulatory and nonstimulatory pMHC systems. For systems with a single stimulatory pMHC, smaller values of f_{MV} would enable the single catch bond to more significantly slow microvillar motion in a fraction of trajectories.

Other models for V_{MV} are also plausible. For example, microvilli could exhibit a "stall force," with applied forces below a threshold having little effect on the velocity and forces above the threshold having a large effect. To this end, we also consider a velocity profile with a Hill-like (sigmoidal) form in the Supplemental Material (text and Supplemental Figure S5). This profile results in an even more pronounced impact of catch bonds due to the inability of nonstimulatory ligands to significantly slow the microvillus on their own.

Assumptions and features of the model

There is compelling evidence for the role of the cytoskeleton in T-cell activation (Yu *et al.*, 2013). However, there is not a clear mechanistic picture of actin-TCR interactions before and during initial TCR-pMHC binding events. In the model, we assume that TCRs undergo diffusive motion at the microvillar tip, where they have been shown to be highly localized (Jung *et al.*, 2016; Kim *et al.*, 2018). We assessed the importance of TCR diffusion by conducting simulations with randomly distributed but immobilized TCRs (Supplemental Figure S1). The results are nearly identical to the case with mobile TCRs, because the microvillar tip is highly confined and contains many TCRs, leaving relatively little space to diffuse. Thus, these results demonstrate that TCR motion within the tip does not have a large impact on the overall response.

The motion of pMHCs is influenced by intracellular interactions likely involving the actin cytoskeleton (Edidin *et al.*, 1991; Kwik *et al.*, 2003; Capps *et al.*, 2004). We assessed the effect of pMHC mobility and found that it influences microvillar motion. When catch bonds were present, faster diffusion of pMHCs produced slower average microvillar motion. Faster diffusion increases the likelihood of stimulatory pMHCs encountering the moving microvillus. Additionally, once stimulatory TCR-pMHC bonds start to slow the microvillus, faster diffusion enhances the transport of other pMHCs from the region around the microvillar tip. This promotes the formation of additional bonds that further stabilize the microvillus.

Immobilized pMHCs were least effective at slowing microvilli. In many contexts, the immobilization of proteins enhances rebinding of recently dissociated complexes due to their prolonged spatial proximity. This can increase the effective on-rate between colocalized proteins (Abel *et al.*, 2012). In our model, TCRs move with the microvillus. Unless the microvillar motion is arrested, initially colocalized TCR-pMHC pairs move apart, even if they are immobilized with respect to their own membrane. This suppresses the potential enhancement of on-rates due to rebinding.

Cai and colleagues showed that the adhesion molecule LFA-1 was excluded from regions in which a microvillus was close to the antigen-presenting surface (Cai *et al.*, 2017). However, it is possible that LFA-1 or other adhesion molecules could play a role in microvillar scanning. LFA-1 is essential for proper T-cell function (Walling and Kim, 2018), and it has been shown to exhibit catch-bond behavior when interacting with its ligand ICAM-1 (Chen *et al.*, 2010). Our model provides a framework to test the potential impact of such interactions, which could influence antigen discrimination, in the future.

Our model shares conceptual features with the molecular clutch model, which is a successful theoretical framework that describes the sensing and response of cells to mechanical properties of their local environments (Chan and Odde, 2008; Elosegui-Artola *et al.*, 2018). It describes the linkage between motor-driven actin retrograde flow and the compliant extracellular substrate of a cell via molecular clutches, which couple the actin to the substrate through binding and force-dependent dissociation. In the molecular clutch model, motors drive the motion of actin, which has a velocity that depends on the force applied by molecular clutches. This is similar to the motion of the microvillus in our model. Molecular clutches bind and unbind the substrate in a force-dependent manner (analogous to TCR-pMHC binding). The substrate is also deformable, with its own inherent stiffness that controls the behavior of the actin flow. The model predicts three actin retrograde-flow regimes that depend on the substrate stiffness and number of molecular clutches: free-flowing, load-and-fail, and stalled. These regimes are similar to the behavior we observe as the number of catch bonds is increased in our system.

In another interesting study, Pielak and coworkers showed that the first few TCR-pMHC binding events increase the on-rate of subsequent TCR-pMHC interactions without changing the dissociation rate (Pielak *et al.*, 2017). This is conceptually similar to our model, in which catch bonds initially slow down scanning microvilli, which promotes additional binding. Pielak and coworkers proposed that morphological changes at the cell–cell interface cause the increased on-rate; morphological changes at the microvillar tip could also impact subsequent binding and antigen discrimination.

A physical mechanism for microvillar stabilization and enhanced antigen discrimination

T-cells exhibit remarkable specificity and sensitivity in their search for antigenic ligands, yet the underlying mechanisms are still not fully understood. A growing body of work has revealed that physical mechanisms involving mechanical forces may play an important role (Hivroz and Saitakis, 2016; Upadhyaya, 2017). In this paper, we have explored feedback between microvillar motion and TCR-pMHC dissociation kinetics. We were intrigued by the results from Cai *et al.* (2017), which revealed that T-cells use microvilli to scan the surfaces of APCs. Additionally, microvilli were stabilized by cognate pMHC, even in the absence of tyrosine kinase signaling, which plays a key role in the early TCR signaling pathway. In light of recent single-molecule studies of TCR-pMHC dissociation kinetics (Liu *et al.*, 2014; Das *et al.*, 2015), we hypothesized that catch-bond kinetics could lead to stabilization. To investigate this idea, we developed a model that captures key biophysical properties of the microvillus–APC interaction but that is simple enough for analysis.

Taken together, our simulation results reveal a purely physical mechanism—the mechanical coupling of microvillar motion and TCR-pMHC binding—that may enhance antigen recognition by T-cells. Forces generated by scanning microvilli provide a means to mechanically "test" TCR-pMHC bonds connecting the microvillar tip to the antigen-presenting surface. If only nonstimulatory TCR-pMHC bonds are present, the microvillar motion constantly increases the force on the bonds and promotes their rupture. Short engagement times would prevent intracellular signaling through the TCR pathway.

In contrast, when a TCR binds to a stimulatory pMHC, the resulting catch bond is able to withstand larger forces, thus allowing it to slow the microvillus and prolong the time spent in the range of forces that enhance its lifetime. For the VSV8 system, forces in the range of ~10–30 pN significantly increase the lifetime of the bond. Thus, with $f_{MV} = 50$ pN in our model, two such bonds can halt the motion of the microvillus if they are aligned so that the force is mostly opposed to the direction of motion. This allows other TCR-pMHC complexes to accumulate and further stabilize the microvillus. As a consequence, the total time that TCRs stay engaged increases substantially when the microvillus is immobilized. This can promote intracellular signaling, starting with phosphorylation of immunoreceptor tyrosine-based activation motifs on the cytoplasmic domain of the TCR complex (Courtney *et al.*, 2018; Siller-Farfán and Dushek, 2018). Because the stimulatory pMHCs are randomly distributed, microvilli stop at random times. Microvilli are immobilized more quickly on average at higher concentrations of stimulatory pMHC because of the increased likelihood of encountering multiple stimulatory pMHCs at once. Faster diffusion of pMHCs also promotes faster immobilization. At very low concentrations of antigenic pMHC, relatively rare encounters can still immobilize a small fraction of the many scanning microvilli and activate the T-cell.

Our results reveal that physical stabilization of microvilli could amplify differences in the response to self and foreign pMHCs, thus enhancing the ability of a T-cell to identify antigens. Other potential advantages that microvilli confer to T-cells are that they enable the scanning of large portions of the APC surface, facilitate contact between TCRs and pMHCs, and may provide protrusive and retractive forces (Cai *et al.*, 2017; Pettmann *et al.*, 2018). Other molecules such as coreceptors, transmembrane phosphatases, and adhesion molecules are also important players in T-cell activation. This is a rich area for future study, and combining experiments and theory

should help to untangle the complex mechano-chemical events leading to antigen discrimination by T-cells. For example, to explore mechanical feedback, it would be useful to conduct imaging studies of the dynamics of T-cell microvilli when interacting with varied concentrations of antigenic pMHCs both immobilized on surfaces and freely diffusing on vesicles or supported lipid bilayers. Additionally, it is interesting to speculate about active search and force generation as a tool in designing synthetic systems for detecting ligands of interest.

REFERENCES
Abel SM, Roose JP, Groves JT, Weiss A, Chakraborty AK (2012). The membrane environment can promote or suppress bistability in cell signaling networks. J Phys Chem B 116, 3630–3640.

Bell GI (1978). Models for the specific adhesion of cells to cells. Science 200, 618–627.

Birnbaum ME, Berry R, Hsiao Y-S, Chen Z, Shingu-Vazquez MA, Yu X, Waghray D, Fischer S, McCluskey J, Rossjohn J, *et al.* (2014). Molecular architecture of the αβ T cell receptor-CD3 complex. Proc Natl Acad Sci USA 111, 17576–17581.

Brameshuber M, Kellner F, Rossboth BK, Ta H, Alge K, Sevcsik E, Göhring J, Axmann M, Baumgart F, Gascoigne N, *et al.* (2018). Monomeric TCRs drive T cell antigen recognition. Nat Immunol 19, 487–496.

Burkhardt JK, Carrizosa E, Shaffer MH (2008). The actin cytoskeleton in T cell activation. Annu Rev Immunol 26, 233–259.

Cai E, Marchuk K, Beemiller P, Beppler C, Rubashkin MG, Weaver VM, Gerard A, Liu T-L, Chen B-C, Betzig E, *et al.* (2017). Visualizing dynamic microvillar search and stabilization during ligand detection by T cells. Science 356, eaal3118.

Capps G, Pine S, Edidin M, Zúñiga MC (2004). Short class I major histocompatibility complex cytoplasmic tails differing in charge detect arbiters of lateral diffusion in the plasma membrane. Biophys J 86, 2896–2909.

Casal A, Sumen C, Reddy TE, Alber MS, Lee PP (2005). Agent-based modeling of the context dependency in T cell recognition. J Theor Biol 236, 376–391.

Chan CE, Odde DJ (2008). Traction dynamics of filopodia on compliant substrates. Science 322, 1687.

Chen W, Lou J, Zhu C (2010). Forcing switch from short- to intermediate- and long-lived states of the αA domain generates LFA-1/ICAM-1 catch bonds. J Biol Chem 285, 35967–35978.

Courtney AH, Lo W-L, Weiss A (2018). TCR signaling: mechanisms of initiation and propagation. Trends Biochem Sci 43, 108–123.

Das DK, Feng Y, Mallis RJ, Li X, Keskin DB, Hussey RE, Brady SK, Wang JH, Wagner G, Reinherz EL, *et al.* (2015). Force-dependent transition in the T-cell receptor β-subunit allosterically regulates peptide discrimination and pMHC bond lifetime. Proc Natl Acad Sci USA 112, 1517–1522.

Depoil D, Dustin ML (2014). Force and affinity in ligand discrimination by the TCR. Trends Immunol 35, 597–603.

Edidin M, Kuo S, Sheetz M (1991). Lateral movements of membrane glycoproteins restricted by dynamic cytoplasmic barriers. Science 254, 1379–1382.

Elosegui-Artola A, Trepat X, Roca-Cusachs P (2018). Control of mechanotransduction by molecular clutch dynamics. Trends Cell Biol 28, 356–367.

Favier B, Burroughs NJ, Wedderburn L, Valitutti S (2001). TCR dynamics on the surface of living T cells. Int Immunol 13, 1525–1532.

Feng Y, Brazin KN, Kobayashi E, Mallis RJ, Reinherz EL, Lang MJ (2017). Mechanosensing drives acuity of αβ T-cell recognition. Proc Natl Acad Sci USA 114, E8204–E8213.

Feng Y, Reinherz EL, Lang MJ (2018). αβ T cell receptor mechanosensing forces out serial engagement. Trends Immunol 39, 569–609.

Fisher PJ, Bulur PA, Vuk-Pavlovic S, Prendergast FG, Dietz AB (2008). Dendritic cell microvilli: a novel membrane structure associated with the multifocal synapse and T-cell clustering. Blood 112, 5037–5045.

Grakoui A, Bromley SK, Sumen C, Davis MM, Shaw AS, Allen PM, Dustin ML (1999). The immunological synapse: a molecular machine controlling T cell activation. Science 285, 221–227.

Hivroz C, Saitakis M (2016). Biophysical aspects of T lymphocyte activation at the immune synapse. Front Immunol 7, 46.

Hogquist KA, Jameson SC, Heath WR, Howard JL, Bevan MJ, Carbone FR (1994). T cell receptor antagonist peptides induce positive selection. Cell 76, 17–27.

Hong J, Ge C, Jothikumar P, Yuan Z, Liu B, Bai K, Li K, Rittase W, Shinzawa M, Zhang Y, et al. (2018). A TCR mechanotransduction signaling loop induces negative selection in the thymus. Nat Immunol 19, 1379.

Hong J, Persaud SP, Horvath S, Allen PM, Evavold BD, Zhu C (2015). Force-regulated in situ TCR-peptide-bound MHC class II kinetics determine functions of CD4+ T cells. J Immunol 195, 3557–3564.

Huang J, Brameshuber M, Zeng X, Xie J, Li Q, Chien Y, Valitutti S, Davis MM (2013). A single peptide-major histocompatibility complex ligand triggers digital cytokine secretion in CD4+ T cells. Immunity 39, 846–857.

Huang J, Zarnitsyna VI, Liu B, Edwards LJ, Jiang N, Evavold BD, Zhu C (2010). The kinetics of two-dimensional TCR and pMHC interactions determine T-cell responsiveness. Nature 464, 932–936.

Jung Y, Riven I, Feigelson SW, Kartvelishvily E, Tohya K, Miyasaka M, Alon R, Haran G (2016). Three-dimensional localization of T-cell receptors in relation to microvilli using a combination of superresolution microscopies. Proc Natl Acad Sci USA 113, E5916–E5924.

Kim H-R, Mun Y, Lee K-S, Park Y-J, Park J-S, Park J-H, Jeon B-N, Kim C-H, Jun Y, Hyun Y-M, et al. (2018). T cell microvilli constitute immunological synaptosomes that carry messages to antigen-presenting cells. Nat Commun 9, 3630.

Kwik J, Boyle S, Fooksman D, Margolis L, Sheetz MP, Edidin M (2003). Membrane cholesterol, lateral mobility, and the phosphatidylinositol 4,5-bisphosphate-dependent organization of cell actin. Proc Natl Acad Sci USA 100, 13964–13969.

Liu B, Chen W, Evavold BD, Zhu C (2014). Accumulation of dynamic catch bonds between TCR and agonist peptide-MHC triggers T cell signaling. Cell 157, 357–368.

Liu Y, Blanchfield L, Ma VP-Y, Andargachew R, Galior K, Liu Z, Evavold B, Salaita K (2016). DNA-based nanoparticle tension sensors reveal that T-cell receptors transmit defined pN forces to their antigens for enhanced fidelity. Proc Natl Acad Sci USA 113, 5610–5615.

Majstoravich S, Zhang J, Nicholson-Dykstra S, Linder S, Friedrich W, Siminovitch KA, Higgs HN (2004). Lymphocyte microvilli are dynamic, actin-dependent structures that do not require Wiskott-Aldrich syndrome protein (WASp) for their morphology. Blood 104, 1396–1403.

O'Donoghue GP, Pielak RM, Smoligovets AA, Lin JJ, Groves JT (2013). Direct single molecule measurement of TCR triggering by agonist pMHC in living primary T cells. eLife 2, e00778.

Pageon SV, Tabarin T, Yamamoto Y, Ma Y, Nicovich PR, Bridgeman JS, Cohnen A, Benzing C, Gao Y, Crowther MD, et al. (2016). Functional role of T-cell receptor nanoclusters in signal initiation and antigen discrimination. Proc Natl Acad Sci USA 113, E5454–E5463.

Pereverzev YV, Prezhdo OV, Forero M, Sokurenko EV, Thomas WE (2005). The two-pathway model for the catch-slip transition in biological adhesion. Biophys J 89, 1446–1454.

Pettmann J, Santos AM, Dushek O, Davis SJ (2018). Membrane ultrastructure and T cell activation. Front Immunol 9, 2152.

Pielak RM, O'Donoghue GP, Lin JJ, Alfieri KN, Fay NC, Low-Nam ST, Groves JT (2017). Early T cell receptor signals globally modulate ligand:receptor affinities during antigen discrimination. Proc Natl Acad Sci USA 114, 12190–12195.

Pullen RH 3rd, Abel SM (2017). Catch bonds at T cell interfaces: impact of surface reorganization and membrane fluctuations. Biophys J 113, 120–131.

Razvag Y, Neve-Oz Y, Sajman J, Reches M, Sherman E (2018). Nanoscale kinetic segregation of TCR and CD45 in engaged microvilli facilitates early T cell activation. Nat Commun 9, 732.

Robbins PF, Li YF, El-Gamil M, Zhao Y, Wargo JA, Zheng Z, Xu H, Morgan RA, Feldman SA, Johnson LA, et al. (2008). Single and dual amino acid substitutions in TCR CDRs can enhance antigen-specific T cell functions. J Immunol 180, 6116–6131.

Sage PT, Varghese LM, Martinelli R, Sciuto TE, Kamei M, Dvorak AM, Springer TA, Sharpe AH, Carman CV (2012). Antigen recognition is facilitated by invadosome-like protrusions formed by memory/effector T cells. J Immunol 1102594.

Sibener LV, Fernandes RA, Kolawole EM, Carbone CB, Liu F, McAffee D, Birnbaum ME, Yang X, Su LF, Yu W, et al. (2018). Isolation of a structural mechanism for uncoupling T cell receptor signaling from peptide-MHC binding. Cell 174, 672–687.

Siller-Farfán JA, Dushek O (2018). Molecular mechanisms of T cell sensitivity to antigen. Immunol Rev 285, 194–205.

Springer TA (1990). Adhesion receptors of the immune system. Nature 346, 425.

Sykulev Y, Joo M, Vturina I, Tsomides TJ, Eisen HN (1996). Evidence that a single peptide-MHC complex on a target cell can elicit a cytolytic T cell response. Immunity 4, 565–571.

Upadhyaya A (2017). Mechanosensing in the immune response. Semin Cell Dev Biol 71, 137–145.

Walling BL, Kim M (2018). LFA-1 in T cell migration and differentiation. Front Immunol 9, 952.

Wofsy C, Coombs D, Goldstein B (2001). Calculations show substantial serial engagement of T cell receptors. Biophys J 80, 606–612.

Yu Y, Smoligovets AA, Groves JT (2013). Modulation of T cell signaling by the actin cytoskeleton. J Cell Sci 126, 1049–1058.